Experimental and computational evidence for stabilising parallel, off-set π[C(=O)N(H)N=C]···π(phenyl) interactions in acetohydrazide derivatives†

Sang Loon Tan,[a] Laura N. F. Cardoso,[b] Marcus V. N. de Souza,[b] Solange M. S. V. Wardell,[c] James L. Wardell*[d] and Edward R. T. Tiekink*[a]

[a] Research Centre for Crystalline Materials, School of Medical and Life Sciences, Sunway University, 47500 Bandar Sunway, Selangor Darul Ehsan, Malaysia

[b] Instituto de Tecnologia em Fármacos Farmanguinhos, FIOCRUZ Fundação Oswaldo Cruz, Rio de Janeiro 21041−250, Brazil

[c] CHEMSOL, 1 Harcourt Road, Aberdeen, AB15 5NY, Scotland, UK

[d] Department of Chemistry, University of Aberdeen, Meston Walk, Old Aberdeen, AB24 3UE, Scotland, UK

E-mail: j.wardell@abdn.ac.uk (JLW); edwardt@sunway.edu.my (ERTT)

Abstract

Parallel, off-set π[C(=O)N(H)N=C]···π(phenyl) interactions are observed in the crystal of (2-thienyl)CH_2CON(H)-N=C(H)Ph, along with more conventional non-covalent interactions. All notable interactions have been analysed by the calculated Hirshfeld surfaces, NCI plots and QTAIM analysis. The π[C(=O)N(H)N=C]···π(phenyl) interactions, whereby the N(H) atom lies over the ring centroid and with the N and C atoms on either side of the N(H) atom closely overlay 1,3-carbon atoms of the phenyl ring, are shown to be attractive. Theory suggests the energy of association provided the π[C(=O)N(H)N=C]···π(phenyl) interaction to the molecular packing to be about 15 kJ/mol, a value similar to that provided by similarly orientated benzene

and pyridine rings. A survey of the literature of related structures suggests comparable interactions occur in approximately 5-6% of crystals where they can potentially occur.

Footnote

† Electronic supplementary information (ESI) available: HRMS spectrum, diagrams of analogous π[C=NN(H)C(=O)]···π(phenyl) interactions occurring literature crystals along with full bibliographic details and selected geometric parameters. CCDC 2036031 contains the supplementary crystallographic data for this paper. For ESI and crystallographic data in CIF or other electronic format see DOI: 10.1039/d0cexxxxxx

Introduction

Non-covalent interactions involving aromatic rings have enormous implications in fundamental biological process pertaining, perhaps most prominently, to the structures of proteins themselves as well as protein-ligand (drug) interactions.[1-5] In addition, these are of obvious importance in supramolecular chemistry as this relates to the packing of molecules in crystals.[6-9]. Recent research on the classical interaction between dimers of benzene molecules reveals interesting observations concerning the energetics of these contacts. First and foremost, is the observation of the edge-to-face (or T-shaped) interaction[10] is associated with the maximum (most stabilising) interaction energy of −11.9 kJ/mol.[11]. The most stable interaction energy for parallel alignments of benzene rings, *i.e.* −11.7 kJ/mol, occurs when the rings are off-set by 1.5 Å; significant interaction energies persist at even greater off-sets.[12] The strength of the arene···arene interaction can be manipulated by systematic chemical substitution[13,14] and/or degree of off-set.[15,16] It should be noted that aromaticity is not the sole criterion for stacking interactions. Thus, studies of cyclohexane···cyclohexane interactions exhibit significant interaction energies.[17] Greater stabilising energies are noted when

cyclohexane···arene interactions are considered, energies which are greater than those associated with benzene···benzene interactions;[17] the off-set between interacting species is also a crucial consideration influencing the relative energy.[18,19]

While not as well-developed as investigations into the various interactions between arene rings,[20] stacking interactions involving heterocyclic rings also have obvious relevance to protein-drug interactions.[21-23] In terms of theory, it is not surprising that the pyridine molecule has attracted most attention.[24,25] One set of calculations show the T-shaped approach between two pyridine molecules, *i.e.* C–H···π(pyridine), results in an interaction energy of –14.9 kJ/mol, being less favourable than stacking interactions (–15.9 kJ/mol).[26] A subsequent study again highlighted the importance of parallel, off-set interactions between pyridine molecules.[27] Arising from a balance between dispersion and repulsion effects between the interacting species, substantial attraction is also apparent at large off-set values (4.5 Å).[27]

Thienyl compounds have found wide uses in the optical and electrical areas,[28] as well as in biological fields.[29] Studies into the latter relate to anti-bacterial,[30] including anti-mycobacterial,[31] anti-inflammatory[32] and anti-cancer activities.[33] In continuation of previous work on the biological activities and structural chemistry of acetohydrazides[34-36] led to the investigation of such derivatives bearing thienyl residues. Thus, four series of 2-thienyl$(CH_2)_n$C(=O)N(R)N=C(H)-Ar [n = 0 or 1; R = H or Me] were prepared and tested as tuberculostatic agents against Mycobacterium tuberculosis H37Rv (ATTC27294)[37,38] and against three cancer cell lines.[39] The crystal structures of two members of this series have been described, namely with Ar = 2-HOC_6H_4 [37] and Ar = 5-nitro-thien-2-yl.[40] It was during these investigations that the parent compound, **1**, Fig. 1, was crystallised. When evaluating the molecular packing in the crystal of **1**, a seemingly unusually close separation between the overlapping planes through the C(=O)N(H)N=C and phenyl residues was detected. Herein, a

crystallographic and extensive computational chemistry study of **1** is described which suggests the unusual contacts is in fact a stabilising π[C(=O)N(H)N=C]···π(phenyl) interaction.

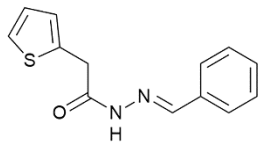

Fig. 1 Chemical diagram for N'-[(1*E*)-phenylmethylidene]-2-(thiophen-2-yl)acetohydrazide (**1**).

Experimental

Chemicals and instrumentation

Melting points were determined on a Buchi apparatus and are uncorrected. Infrared spectra were recorded on a Thermo Nicolet Nexus 670 spectrophotometer in KBr. NMR spectra were recorded on a Bruker Avance 400 machine operating at 400.00 MHz (^{1}H) and 100.0 MHz (^{13}C{^{1}H}) in DMSO-d_6 solution. Thin layer chromatography (TLC) plates, coated with silica gel, were run in chloroform / methanol mixtures and spots were developed using ultraviolet light. The HRMS spectrum was measured on a Bruker Compact instrument with an ESI source and in the positive mode.

Synthesis of *N′*-[(*E*/*Z*)-phenylmethylene]-2-(thien-2-yl)acetohydrazide (1)

Initially, 2-(thien-2-yl)acetohydrazide was prepared. A solution of methyl 2-thienylacetate (1.0 g, 1.0 equiv.) and hydrazine hydrate (2.8 ml, 1.5 equiv., aqueous solution 55%) in EtOH (5.0 ml) was stirred for 1 h at 80 °C, then concentrated under reduced pressure. The residue was successively washed with cold EtOH (2 × 10 ml) and Et_2O (2 × 10 ml), and recrystallized from EtOH as a yellow solid (0.75 g, 75%). M.pt: 90–91 °C. A solution of 2-(thien-2-yl)acetohydrazide (0.2 g, 1.0 equiv.) and benzaldehyde (1.2 equiv.) in EtOH (2.0 ml) was

stirred at room temperature until TLC indicated reaction was complete. The reaction mixture was concentrated under reduced pressure and the residue was washed with cold Et_2O (2 × 10 mL) and recrystallised from ethanol. Yield: 0.18 g, 52%; white solid; M.pt: 135–137°C. HRMS *m/z*: 267.0556 for $C_{13}H_{12}N_2OS$+Na (calcd. 267.0568). The peak at 511.1219 is the [2M.Na]+ peak; the spectrum is shown in ESI† Figure S1.

Spectroscopic characterisation

IR λ_{max} (cm^{-1}; KBr): 3178 (N–H); 1667 (C=O); 1608 (C=N). ^{1}H NMR (400 MHz; DMSO-d_6) δ: 11.63 (0.33H, s, NH, *anti*-conformer), 11.45 (0.66H, s, NH, *syn*-conformer), 8.21 (0.33H, s, C(H)=N, *anti*-conformer), 8.02 (0.66H, s, C(H)=N, *syn*-conformer), 7.76–7.36 (5H, m, H-9 to H-13), 7.35 (1H, dd, J = 5.0 & 1.5 Hz, H-2), 6.99–6.97 (1H, m, H-4), 6.96–6.94 (1H, m, H-3), 4.19 (1.33H, s, CH_2, *syn*-conformer), 3.78 (0.66H, s, CH_2, *anti*-conformer). ^{13}C NMR (100 MHz, DMSO-d_6) δ: 171.1 (CO, *anti*-conformer), 165.6.0 (CO, *syn*-conformer), 147.4 (C(H)=N, *anti*-conformer), 143.6 (C(H)=N, *syn*-conformer), 137.2 (C-8), 134.6 (C-1), 130.5, 130.3 & 129.3 (C-9, C-11 & C-13), 127.5, 127.3, 127.2, 126.9 (C-2, C-3, C10 & C12), 124.8 (C-4), 35.3 (C5, *syn*-conformer), 33.2(CH_2, *anti*-conformer).

X-ray crystallography

Intensity data for a colourless crystal of **1** (0.08 x 0.10 x 0.60 mm) were measured at 100 K on a Bruker-Nonius FR591 rotating anode fitted with a rotating anode; MoKα radiation (λ = 0.71073 Å) so that data completeness was made at θ_{max} = 25.2°. The data processing employed COLLECT[41] and DENZO,[42] and the absorption correction, based on multiple scans, was accomplished with SADABS.[43] The structure was solved by direct methods[44] and the refinement was by full-matrix least squares on F^2 with anisotropic displacement parameters for all non-hydrogen atoms.[45] The C-bound hydrogen atoms were placed on stereochemical

grounds and refined with fixed geometries while the N-bound hydrogen atom was located from a difference map and refined with N–H = 0.88±0.01 Å. A weighting scheme of the form $w = 1/[\sigma^2(F_o^2) + (0.049P)^2 + 3.244P]$ where $P = (F_o^2 + 2F_c^2)/3$ was introduced in the refinement. Owing to poor agreement, one reflection, *i.e.* (1 1 0), was omitted from the final cycles of refinement. The programs WinGX,[46] ORTEP-3 for Windows,[47] PLATON[47] and DIAMOND[48] were also used in the study.

Crystal data for **1** at 100 K: $C_{13}H_{12}N_2O$ S, M = 244.31, monoclinic, $C2/c$, a = 21.7010(7) Å, b = 6.1737(2) Å, c = 20.5621(7) Å, β = 120.251(1)º, V = 2379.68(14) Å^3, Z = 8, D_x = 1.364 g cm^{-3}, μ = 0.256 mm^{-1}, no. reflections measured = 14482, no. unique reflections = 2733, no. reflections with $I \geq 2\sigma(I)$ = 2135, R (obs. data) = 0.042, R_w (all data) = 0.111.

Computations

The geometry optimisation of **1** was performed at the Becke Three-parameter Lee-Yang-Parr Hybrid Functionals B3LYP[49]/Def2TZVP[50,51] level of theory through Gaussian16[52] using the experimental coordinates as the input. The Hirshfeld surface analysis was performed using Crystal Explorer 17 (ref. [53]) based on the methods reported in the literature.[54] The d_{norm} map was obtained by calculating the normalised distances from the contact points on the surface to the nearest nucleus inside (d_i) or outside (d_e) the surface upon the adjustment of all X–H bond length to their neutron-derived values.[55] The molecular electrostatic potential map (MEP) was obtained by mapping the electrostatic potential over the Hirshfeld surface using the Becke Three-parameter Lee-Yang-Parr Hybrid Functionals B3LYP[49] with the 6-31G(*d*,*p*) basis set[56,57] while the intermolecular interaction energies were calculated using the dispersion corrected CE-B3LYP/6-31G(*d*,*p*) model;[58] both sets of calculations o were executed through the *Tonto* quantum modelling package[59] integrated in Crystal Explorer 17.[53] The natural bonding orbital[60,61] (NBO) analysis, at the B3LYP[49]/Def2TZVP[50,51] level of theory was

calculated with Gaussian16.[52] The combined quantum theory of atoms in molecules (QTAIM) and non-covalent interaction plot (NCIPLOT) were performed with the Multiwfn program[62] based on topological analysis of electron densities[63-65] as well as the visualisation index derived from the reduced density gradient.[66,67] The resulting isosurfaces were visualised using the VMD molecular Graphics Viewer.[68]

Results and discussion

Compound **1** was synthesised from the 1:1 condensation reaction between 2-(thien-2-yl)acetohydrazide and benzaldehyde. The notable feature of the spectroscopic analysis is the appearance in DMSO-d_6 solution of both *syn*- and *anti*-dispositions for the amide C(=O)–NH residue; the molecule adopts an *E*-configuration about the imine-C=N bond. This is manifested primarily in the appearance of distinct resonances for the amine-H, imine-C(H)=N and methylene-H protons in the ^{1}H NMR, and for the carbonyl-, imine- and methylene-C nuclei in the $^{13}C\{^{1}H\}$ NMR. The integration of the relevant ^{1}H NMR proton resonances indicates the most prominent conformer for **1** is the one with the *syn*-disposition of the amide residue, in a 2:1 ratio. These observations are consistent with previous NMR spectral and theoretical studies of acetohydrazides, RC(=O)N(H)N=CHR′, which indicate in solution that they generally exist mainly or solely as mixtures of *syn*- and *anti*-conformers.[69-72] Computational chemistry calculations on representative molecules show the *syn*-isomer is more stable, *e.g.* HC(=O)N(H)N=CH(2-pyridyl) (5.06 kJ/mol) and PhC(=O)N(H)N=CH(2-pyridyl) (15.28 kJ/mol) by relatively little energy.[73] The absence, or very low proportions, of forms involving the *Z*-conformer about the imine-C=N bond is a consequence of steric hindrance. The NMR study conducted on **1** follows these general findings.

Molecular structure

The experimental molecular structure of **1** is shown in Fig. 2. In keeping with the spectroscopic study, the configuration about the imine-C=N bond is *E*, and the disposition of the amide group is *syn*. The molecule is twisted about the C5–C6 bond as seen in the C1–C5–C6–N1 torsion angle of -90.79(19)°, indicative of a -syn-clinal (-sc) conformation, and in the dihedral angle of 86.82(11)° formed between the aromatic rings, indicative of a near to perpendicular orientation. The central residue comprising the O1, N1, N2, C6 and C7 atoms is effectively planar, exhibiting a r.m.s. deviation of 0.0105 Å with a maximum deviation of 0.0179(12) Å for the N1 atom; the appended methylene-C5 atom lies 0.098(5) Å out of the plane to the same side as the N1 atom, and the phenyl-C8 atom lies 0.067(3) Å to the other side. The crucial bond lengths are summarised in Table 1: these are suggestive of delocalisation of π-electron density of the planar, central residue.

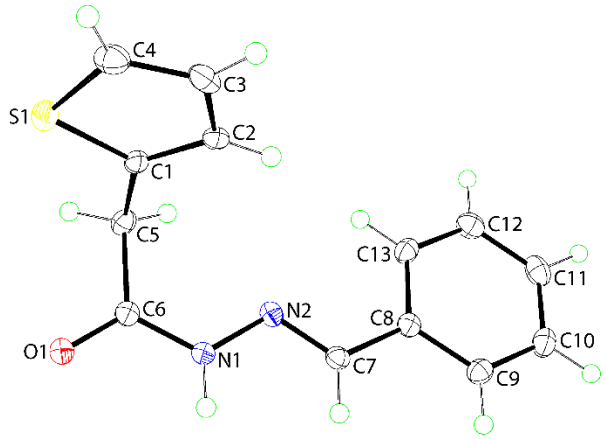

Fig. 2 The molecular structure of **1** showing atom-labelling scheme and displacement parameters at the 50% probability level.

Table 1 Key geometric parameters (Å, º) for the experimental (X-ray) and geometry optimised structures of **1**

Parameter	X-ray	Optimised
N1–N2	1.378(2)	1.351

C6–O1	1.236(2)	1.214
C6–N1	1.351(2)	1.378
C7–N2	1.282(2)	1.279
O1–C6–N1	120.41(16)	119.4
O1–C6–C5	120.98(16)	123.0
N1–C6–C5	118.50(16)	117.6
N2–N1–C5	121.20(15)	124.4
N1–N2–C7	115.29(15)	117.7
O1,N1,N2,C5,C7/S1,C1-C4	80.97(11)	70.1
O1,N1,N2,C5,C7/C8-C13	5.9(2)	3.0
S1,C1-C4/C8-C13	86.82(5)	73.1

The geometry optimised structure for **1** was also calculated; selected derived geometric parameters are collated in Table 1. There is a close concordance between the molecules as illustrated in Fig. 3 with relatively minor differences in conformation. It is instructive to evaluate differences in the key bond lengths within the central C(=O)N(H)N=C residue, most notably the shortening of the N1–N2 and C6–O1 bonds in the optimised molecule with a concomitant lengthening of the C6–N1 bond, consistent with reduced delocalisation of π-electron density over the residue in the gas-phase.

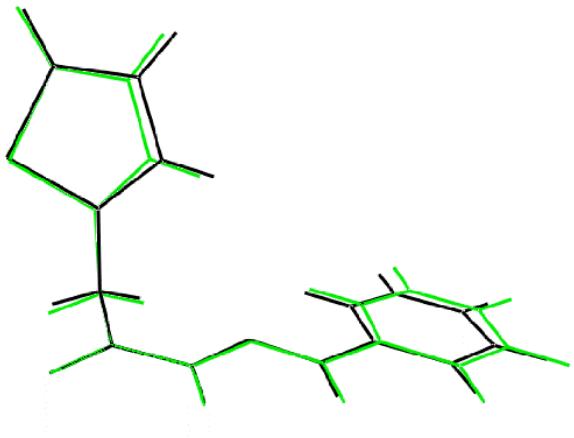

Fig. 3 Overlay diagram for the experimental (black image) and geometry-optimised (green image) structures of **1**.

Molecular packing

In addition to conventional hydrogen bonding, a number of other non-covalent interactions were identified in the crystal of **1**, based on an analysis conducted on the geometric criteria assumed in PLATON.[47] The *syn*-disposition of the amide-H and carbonyl-O atoms facilitates the formation of an eight-membered $\{\cdots OCNH\}_2$ synthon *via* amide-N–H···O(amide) hydrogen bonding. Directional interactions between the dimeric aggregates within the three-dimensional architecture include thien-2-yl-C–H···O(amide), thien-2-yl-C–H···π(phenyl), methylene-C–H···π(thien-2-yl) and phenyl-C···π(thien-2-yl) interactions; a view of the unit-cell contents is given in Fig. 3(a).

Table 2 A summary of the geometric parameters (Å, º) characterising the key interatomic contacts (A–H···B) in the crystal of **1**

Contact	H···B	A···B	A–H···B	Symmetry operation

N1–H1n···O1	1.98(2)	2.851(2)	175(2)	1½-*x*, -½-*y*, 1-*z*
C2–H2···O1	2.43	3.277(2)	148	*x*, 1+y, *z*
C4–H4···Cg(C8-C13)	2.78	3.531(2)	137	½+*x*, ½-*y*, ½+*z*
C5–H5b···Cg(S1,C1-C4)	2.69	3.564(2)	147	1½-*x*, -½+*y*, 1½-z
C9–H9···Cg(S1,C1-C4)	2.82	3.766(2)	177	1½-*x*, 1/2-*y*, 1-*z*

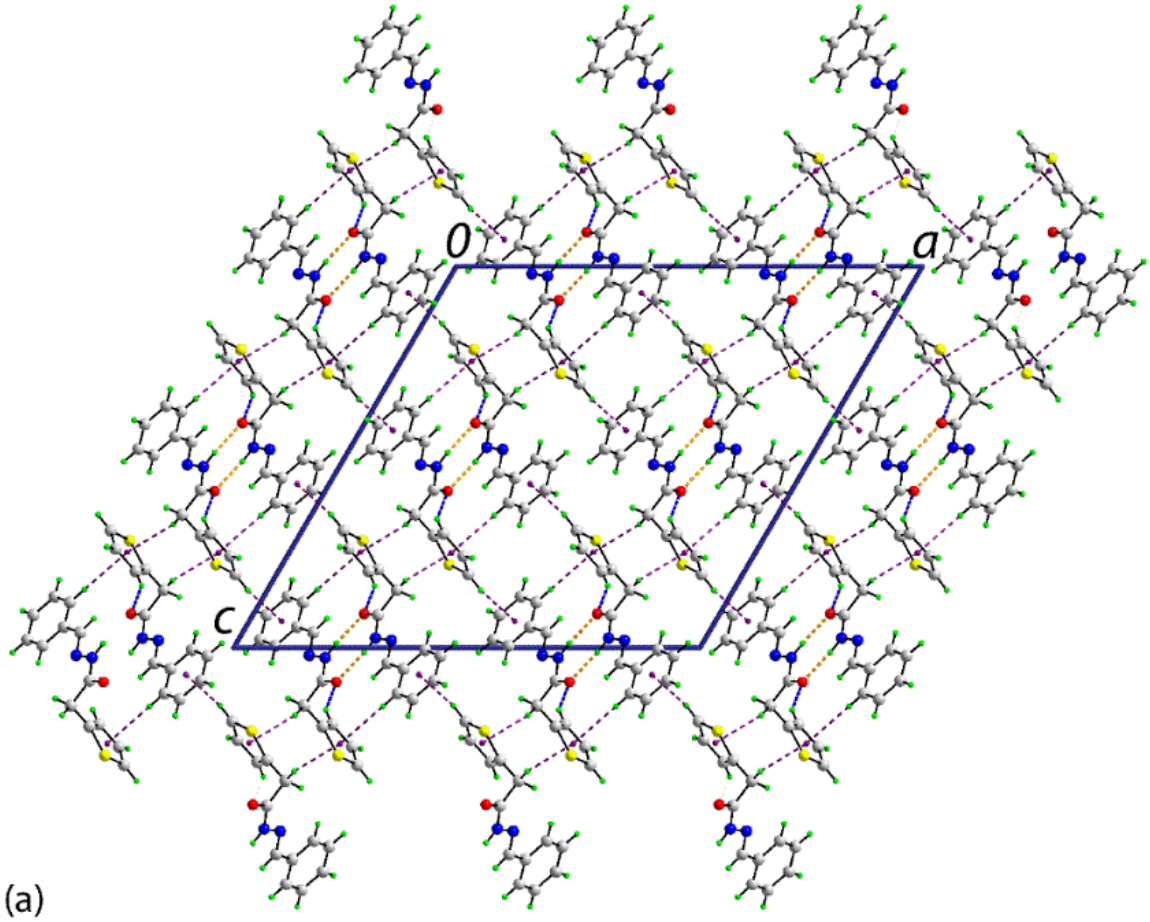

(a)

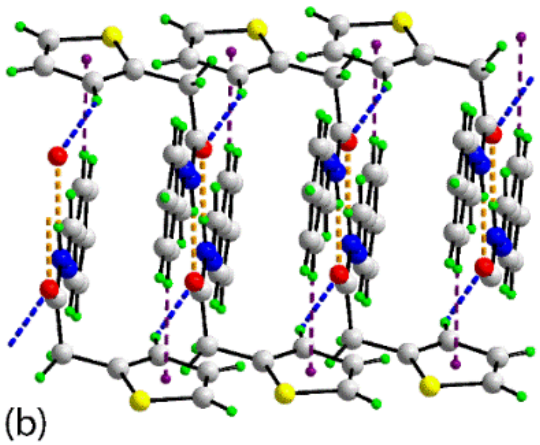

(b)

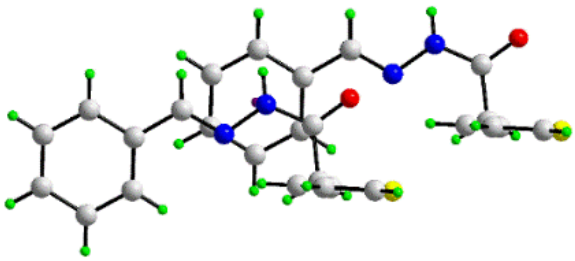

(c)

Fig. 4 Images of the molecular packing in **1**: (a) a view of the unit-cell contents in projection down the *b*-axis, (b) view of the supramolecular aggregation along the *a*-axis and (c) a detailed view of the overlay of the C(=O)N(H)N=C and phenyl residues.

Of particular interest in the packing are the interactions along the *a*-axis. As shown in Fig. 3(b), apparent in this direction are thien-2-yl-C–H···O(amide) and phenyl-C···π(thien-2-yl) interactions as well as the seemingly parallel orientation of the phenyl rings. However, rather than close π(phenyl)···π(phenyl) contacts, more prominent are ostensible π[C(=O)N(H)N=C]···π(phenyl) interactions as highlighted in Fig. 3(c). Here, the amide-N atom lies plumb to the ring centroid of the phenyl ring with the N···Cg(phenyl) separation = 3.27 Å, compared with a van der Waals separation of 3.45 Å being the sum of the van der Waals radius of nitrogen (1.55 Å)[74] and a phenyl ring (1.90 Å).[75] Also notable is that the imine-C and amide-C atoms of the C(=O)N(H)N=C fragment lie over 1,3-C atoms of the phenyl ring with C···C separations of 3.295(3) and 3.347(2) Å, respectively. The dihedral angle between the C_2N_2O and phenyl residues is 5.73(10)°. The cited geometric parameters resemble those that might be observed in a regular parallel, off-set π(phenyl)···π(phenyl) interaction and forms the primary focus of subsequent investigations. It is noted the angles about the N1 atom sum to 359.9° consistent with conjugation through the C(=O)N(H)N=C residue, mentioned above, and is suggestive the presence of a significant π-hole on the nitrogen atom.[76-79] Finally, as the N1 atom sits atop of the phenyl ring centroid, the off-set between the π-systems is close to 1.39 Å, being the separation between the ring centroid and atom C11.

Hirshfeld surface analysis

The Hirshfeld surface analysis was performed to understand more fully the nature of supramolecular interactions present in the crystal. As shown in Fig. 5, the d_{norm} mapping

reveals there are several close contacts with contact distances shorter than the sum of van der Waals radii (ΣvdW) as indicated by the presence of red spots on the mapped surface. The most intense red spots arise from the amine-H1n···O1(amide) hydrogen bond with the d_{norm} contact distance of 1.85 Å being significantly shorter than the ΣvdW radii by about 0.77 Å,[47] Table 3. Other red spots are attributed to thien-2-yl-H2···O1(carbonyl), amide-C6···C13(phenyl) and methylene-H5b···C2(thien-2-yl) contacts with their intensity being proportional to $\Delta|d_{norm} - \Sigma vdW|$ of 0.287, 0.105 and 0.040 Å, respectively.

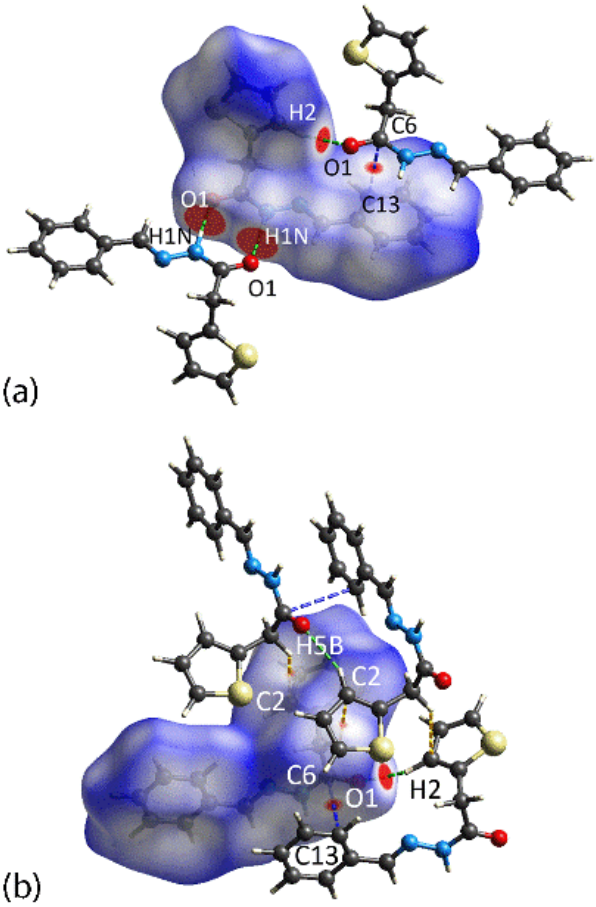

Fig. 5 Two views of the Hirshfeld surface for **1** mapped over d_{norm} within the range -0.0518 to 1.0300 arbitrary units.

Table 3 A summary of the d_{norm} contact distances for interactions present in the crystal of **1** as computed through an analysis of the calculated Hirshfeld surface. The X–H distances have been adjusted to their neutron values

Intermolecular Contact	Distance (Å)	ΣvdW (Å)	$\Delta\lvert d_{norm} - \Sigma vdW\rvert$ (Å)	Symmetry Operation
N1–H1n···O1	1.85	2.61	0.77	1½-*x*, -½-*y*, 1-*z*
C2–H2···O1	2.32	2.61	0.29	*x*, 1+*y*, *z*
C6···C13	3.30	3.40	0.11	*x*, 1+*y*, *z*
C5–H5b···C2	2.75	2.79	0.04	1½-*x*, -½+*y*, 1½-*z*

The C6 atom in the acetohydrazide fragment [O1=C6–N1(H1n)–N2=C7] and C13 in the phenyl ring (C8-C13) of the symmetry related molecule (see Table 3) has been identified on the calculated Hirshfeld surface. While the adjacent the N1···Cg(phenyl) and N2···C11 contacts do not appear, the putative π[C(=O)N(H)N=C]···π(phenyl) interaction is supported by shape the complementarity revealed through the Hirshfeld surface mapped over the curvedness property between the two overlapped fragments, as highlighted in Fig. 6.

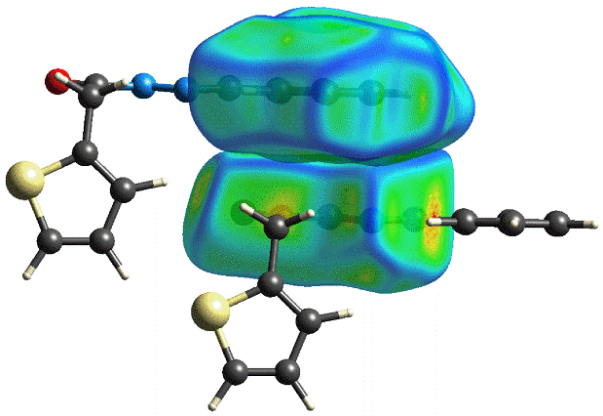

Fig. 6. The Hirshfeld surface for **1** mapped with curvedness for the phenyl ring (C8-C13) (top) and acetylhydrazide residue [O1=C6–N1(H1n)–N2=C7], highlighting the shape complementarity between the two molecular fragments.

Computational chemistry

In an attempt to establish further proof for the π[C(=O)N(H)N=C]···π(phenyl) interaction in the crystal of **1**, several computational methods including NBO (Natural Bond Order) analysis, MEP (Molecular Electrostatic Mapping) mapping, QTAIM (Quantum Theory of Atoms In Molecules) and NCI (Non-Covalent Interaction) plot calculations were employed to study the close contacts between the atoms of the interacting acetohydrazide and phenyl fragments.

Initially, an NBO analysis was conducted for the optimised molecule (see above) to verify the conjugation along the O1=C6–N1(H1n)–N2=C7 fragment with results presented in Table 4. Through the calculation of the hybrid composition of the corresponding NBO's for the acetohydrazide fragment, the expected sp^2 hybridisation is clearly evident for the O1, C6 and C7 atoms. Of interest is the composition of the of orbitals for the nominally sp^3-N1 and sp^2-N2 atoms. The calculations show clear evidence of sp^2-character about N1 in the bonds it forms with N2 and C1. Complementing this are deviations from sp^2-character in the bonds formed between the N2 atom and each of N1 and C7. The obtained results indicate the molecule exhibits significant conjugation along the heteroatoms of the O1=C6–N1(H1n)–N2=C7 fragment.

Table 4 The hybrid composition of natural bonding orbitals within the O1=C6–N1(H1n)–N2=C7 fragment

X–Y	X	Y

	Overall occupancy (%)	% *s*	% *p*	Overall occupancy (%)	% *s*	% *p*
O1=C6	63.6	39.4	60.0	36.4	34.3	65.7
N1–C6	62.4	37.4	62.3	37.6	30.3	69.6
N1–N2	53.3	33.3	66.6	46.7	24.4	75.2
N2=C7	59.3	41.6	57.9	40.7	34.2	65.7

Despite the restricted flow of electrons along the conjugated bond, MEP mapping shows this phenomenon does not significantly affect the interaction between the acetohydrazide residue and phenyl ring, as these structural fragments exhibit complementary (opposite) electrostatic potential charges that leads to attraction between them, as illustrated in Fig. 7.

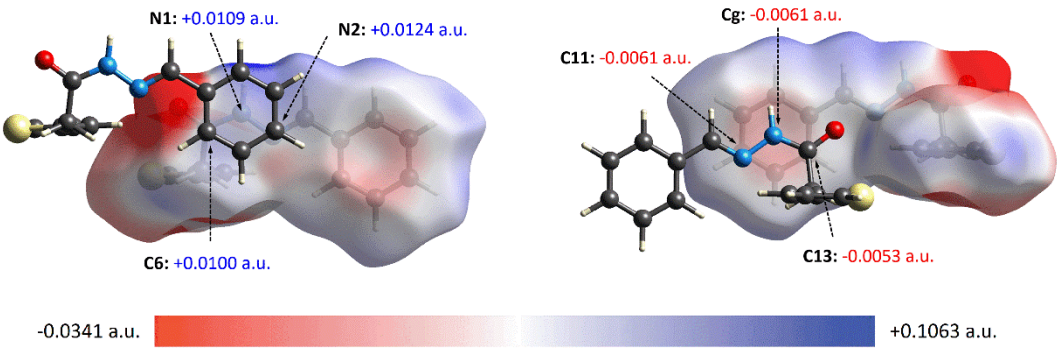

Fig. 7 The two views of the MEP map calculated for **1**, showing the electrostatic potential charges of the interacting atoms in the O1=C6–N1(H1n)–N2=C7 and phenyl ring fragments.

The NCI plot and QTAIM analysis further justifies the existence of the conjugated π[C(=O)N(H)N=C]···π(phenyl) interaction. Referring to Fig. 8, there is a considerable large,

localised green domain appearing between the fragments in the NCI plot, indicative of a weakly attractive interaction, along with the presence of bond critical points connecting the C6···C13, N1···C11 and N2···C11 pairs of atoms. These results signify the formation of attractive interaction between these residues.

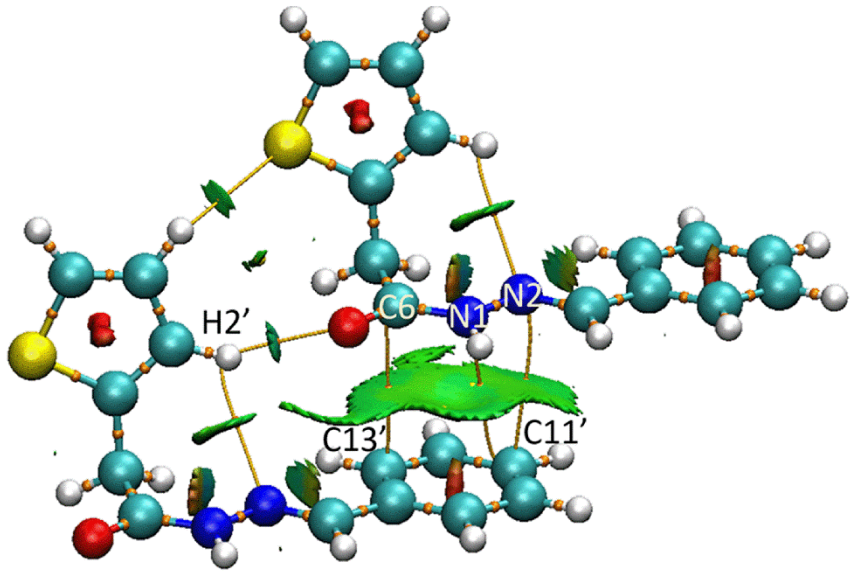

Fig. 8 A diagram combining the NCI plot and QTAIM analysis between the stacking regions of **1**, showing the attractive interaction represented by the green domain (indicative of weak attraction; the blue and red domains are indicative of strong attraction and strong repulsion, respectively) along with interactive paths characterised by the bond critical points. For the NCI isosurface, the cutoff is set as RDG = 0.5 a.u. and colour scale is within -0.4 < ρ < 0.04 a.u.

Quantification of intermolecular contacts

Having established the presence of conjugated π[C(=O)N(H)N=C]···π(phenyl) interaction in **1**, the pairwise molecules were subjected to quantitative calculation of the interaction energy (E_{int}) in order to estimate the strength of this and other interactions prominent in the crystal; data are collated in Table 5. The calculations show the E_{int} for the conjugated π···π interaction together with the C2–H2···O1 contact is about −33.3 kJ/mol, a value relatively weaker than

the pair of conventional N1–H1n···O1 hydrogen bonds within a $\{\cdots OCNH\}_2$ synthon with an E_{int} of −82.6 kJ/mol, Table 5.

Table 5 Interaction energies (kJ/mol) for close contacts present in the structure of **1**

Close contact	E_{ele}	E_{pol}	E_{disp}	E_{rep}	E_{tot}	Symmetry operation
$\{$N1–H1n···O1$\}_2$	−120.4	−18.1	−15.7	71.6	−82.6	1½-*x*, -½-*y*, 1-*z*
C2–H2···O1 + C6···C13 + N1···*Cg*(C8-C13) + N2···C11	−25.1	−4.7	−37.1	33.6	−33.3	*x*, 1+*y*, *z*
C5–H5b···C2	−12.3	−1.4	−23.9	16.5	−21.1	1½-*x*, -½+*y*, 1½-*z*

The cooperation of the π[C(=O)N(H)N=C]···π(phenyl) and C2–H2···O1 interactions between molecules serves to highlight that intermolecular contacts between molecules do not operate independently in crystals and to the difficulty of ascertaining the contributions of specific contacts. A closely related system available for comparison is the idealised pyridine-benzene dimer.[25-27] Various orientations and off-sets for parallel interactions for this system have been evaluated computationally.[27] For a parallel ring off-set between the rings comprising the pyridine-benzene dimer of about 1.39 Å, the energy of stabilisation between the rings is approximately 15.2 kJ/mol.[27] As indicated above, the off-set between the π-systems in **1** is about 1.39 Å and thus this energy of stabilisation can be a preliminary approximation for the energy of stabilisation provided by the π[C(=O)N(H)N=C]···π(phenyl) interaction.

Literature precedents

In order to assess the prevalence of analogous π[C=NN(H)C(=O)]···π(phenyl) interactions in the crystallographic literature, a search of the Cambridge Structural Database[80] (CSD version 5.42 plus two updates) was conducted employing ConQuest (version 2021.1.0).[81] The CSD was searched for crystals containing both CC=NN(H)C(=O)C fragments along with an arene ring. The primary search criterion was geometric in that the separation between the central nitrogen atom of the C=NN(H)C(=O) fragment and the ring centroid of the arene ring was less than 3.45 Å, a value based on the sum of the van der Waals radii for the interacting species.[74,75] Additional criteria were that the three-dimensional coordinates were available, $R \leq 0.075$, there were no errors or disorder, no ions, single crystal data only for solely organic molecules. This resulted in 73 hits after the removal of six duplicates. The bibliographic details, key geometric parameters and structural diagrams of the supramolecular aggregates featuring π[C=NN(H)C(=O)]···π(arene) interactions in the 73 hits are shown in ESI† Tables 1 and 2. The first noteworthy observation to be made before discussing more specific details is that in all hits there is a close superimposition of the carbon atoms of the C=NN(H)C(=O) fragment over 1,3-carbon atoms of the arene ring as observed in **1**.

The chemical diagrams for the specific molecules to be discussed in the following are given in Fig. 9. The first distinguishing feature between the 73 structures is the configuration of the amide group. Only in six examples are the amide-O and H atoms *syn*, as observed in **1**. Two examples, *i.e.* **s1** (ref. [82]) and **s2**,[83] associate *via* a π[C=NN(H)C(=O)]···π(phenyl) interaction to form a centrosymmetric dimer, as illustrated in Fig. 10a for **s1**; this molecule is also notable for being the only example among the 73 to be discussed whereby the amide group is incorporated within a ring. As for **1**, linear chains are found in the remaining examples, **s3**-**s6** (refs [84-87]).

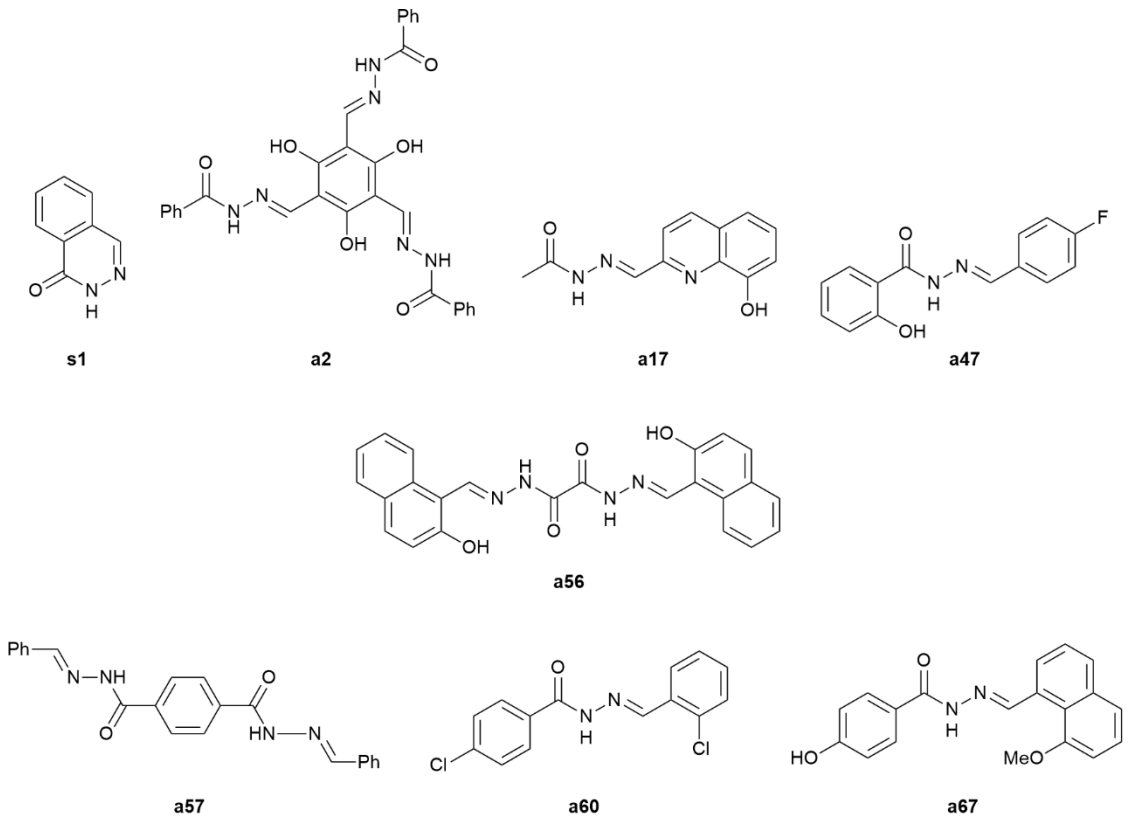

Fig. 9. Chemical diagrams for selected literature acetohydrazide derivatives.

The remaining 67 aggregates feature the amide group with an *anti*-configuration. The molecules in **a1** (ref. [88]) and **a2** (ref. [89]) have the common feature that two molecules comprise the asymmetric-unit and these associate by a single π[C=NN(H)C(=O)]···π(phenyl) interaction to form a non-symmetric two-molecule aggregate, as illustrated in Fig. 10b for **a2**, which is notable for having three C=NN(H)C(=O) residues as well as three phenyl rings available to form these interactions. There are 32 crystals featuring centrosymmetric dimers, namely **a3**-**a34** (refs. [90-121]) with the dimer formed by **a17** (ref. [104]) illustrated in Fig. 10c. It is noted that only one of the two C=NN(H)C(=O) residues of **a34** (ref. [121]) forms the π[C=NN(H)C(=O)]···π(phenyl) interaction. A further clue on the likelihood for molecules to self-associate *via* π[C=NN(H)C(=O)]···π(phenyl) interactions in their crystals is indicated by the number of crystals among this sub-set that feature multiple molecules in the asymmetric-unit. Thus, for each of **a4**,[91] **a9**,[96] **a12**,[99] **a14**,[101] **a17**,[104] **a20**,[107] **a26** (ref. [113]) and **a29**,[116] two

molecules comprise the asymmetric-unit yet only one of these self-associates to form the two-molecule aggregate. This theme continues for **a8**,[95] for which only one of the four independent molecules forms a dimer.

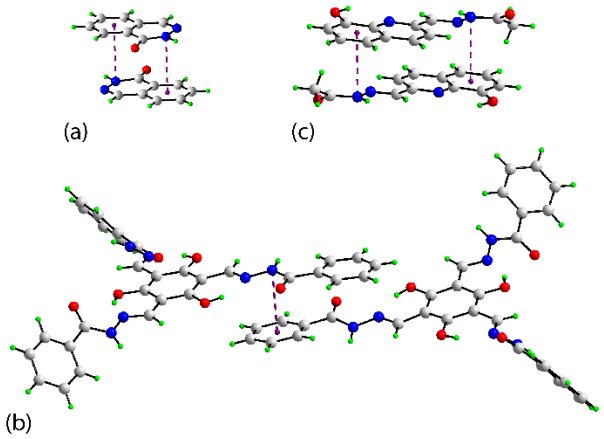

Fig. 10. Images of π[C=NN(H)C(=O)]···π(phenyl) interactions leading to dimeric aggregates in (a) **s1**, (b) **a2** and (c) **a17**; refer to Fig. 9 for the chemical diagrams of the participating molecules.

The remaining aggregates to be discussed are supramolecular chains. The chains in crystals **a35**-**a55** (refs [121-139]) have a linear topology as exemplified by **a47** (ref. [132]) in Fig. 11a. In this assembly, each molecule forms, on average, one donor and one acceptor π[C=NN(H)C(=O)]···π(phenyl) interaction. Variations are noted in **a56** (ref. [140]) and **a57** (ref. [141]). As seen in Fig. 11b, each of the C=NN(H)C(=O) residues in **a56** participates in a π[C=NN(H)C(=O)]···π(phenyl) interaction so that on average each molecule forms two donor and two acceptor interactions within in a linear chain. Two C=NN(H)C(=O) residues are also present in centrosymmetric **a57** and each of these participates in a π[C=NN(H)C(=O)]···π(phenyl) interaction with a common (central) phenyl ring to a generate a linear supramolecular chain, illustrated in Fig. 11c. The distinguishing feature of the linear chains found in **a58**-**a66** (refs [142-150]) is the presence of hydrogen bonded molecules on the

periphery of the chain, highlighting the concept of cooperativity of intermolecular interactions;[151] an example is shown in Fig. 11d for **a60**. The final chain found for **a67** (ref. [152]) is distinguished by having a zigzag topology, Fig. 11e.

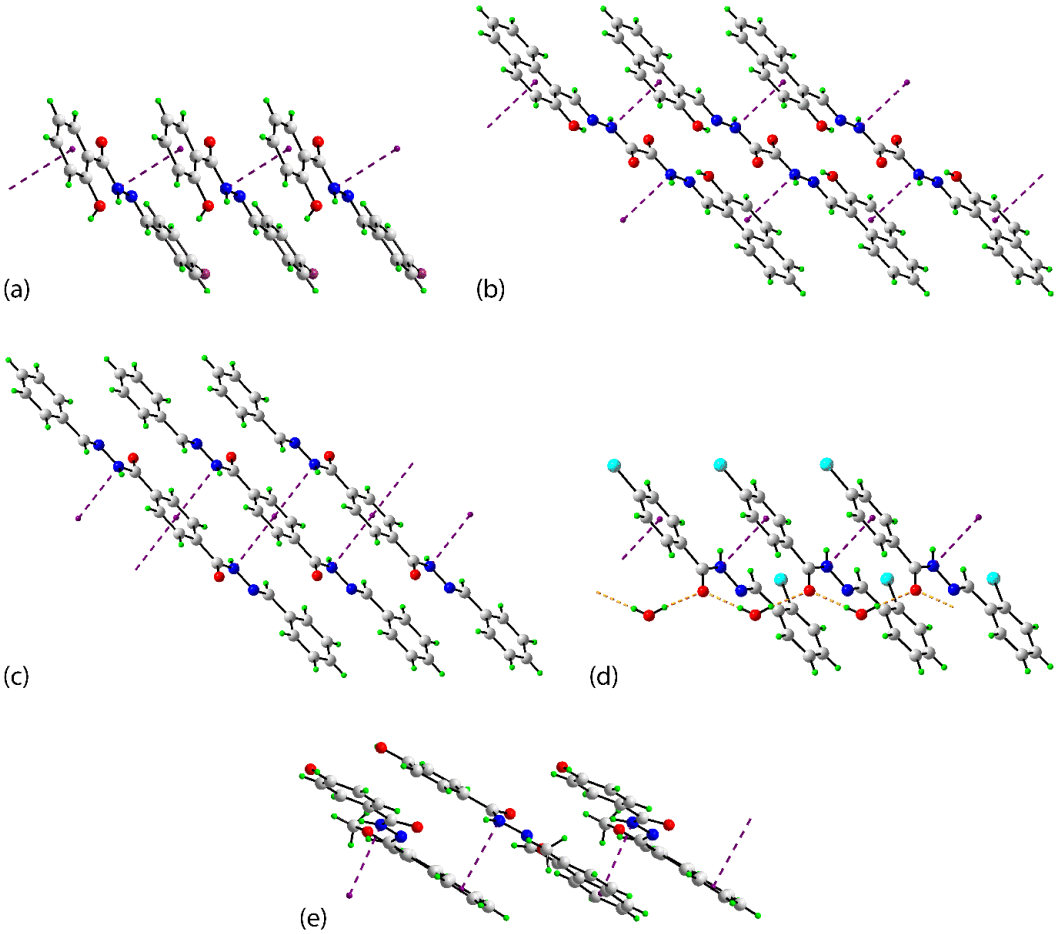

Fig. 11. Images of π[C=NN(H)C(=O)]···π(phenyl) interactions leading to supramolecular chains in (a) **a47**, (b) **a56**, (c) **a57**, (d) **a60**.H_2O and (e) **a67**; refer to Fig. 9 for the chemical diagrams of the participating molecules.

A pair of polymorphs is noted among the literature precedents, namely for **a53** (ref. [137]) and **a54**.[138] A polymorph is also known for each of **a3**,[111] and **a5**,[153] but neither of these features a π[C=NN(H)C(=O)]···π(phenyl) interaction in the crystal.

A brief mention of the geometric parameters characterising the π[C=NN(H)C(=O)]···π(phenyl) interactions for the literature structures as listed in ESI† Tables 1 and 2 is apposite. From the data collated therein, the shortest separation between the N1 atom and the ring centroid of the arene ring is 3.26 Å in **a55**,[139] with several examples right at the van der Waals threshold, *e.g.* **a5**,[92] **a32** (ref. [119]) and **a63**.[147] The average separation computes to 3.39 Å with the median value also being 3.39 Å. The smallest dihedral angle between the π-systems of 0.8° is found in each of **a56** (ref. [140]) and **a3**,[111] with the widest angle of 20.6° noted in **a12**.[99] However, there is no correlation between the distance between planes and dihedral angle with a plot between these parameters having r^2 = 0.02. The greatest deviation from 360° of sum of the angles about the N1 atom is 358.2° in **s4**.[85]

Finally, in order to gauge the propensity of forming π[C=NN(H)C(=O)]···π(phenyl) interactions in crystals, a search of the CSD was performed employing the criteria outlined above without the N1···ring centroid distance restraint; the arene ring was not constrained to be connected to the C=NN(H)C(=O) fragment. This survey suggests that π[C=NN(H)C(=O)]···π(phenyl) interactions form in just over 5.7% of crystals where they can potentially form.

Conclusions

Experimental and computational evidence for an attractive π[C=NN(H)C(=O)]···π(phenyl) interaction in a crystal of acetohydrazide derivative, **1**, is revealed. An estimate of the energy of stabilisation provided by this association in the crystal of **1** is about 15 kJ/mol. Analogous π[C=NN(H)C(=O)]···π(phenyl) interactions occur in about 5-6% of crystals where the potential to form is present.

Conflicts of interest

The authors declare no competing financial interest.

Acknowledgements

J.L.W. thanks CAPES (Brazil) for support. The authors gratefully acknowledge Sunway University Sdn Bhd (Grant numbers GRTIN-IRG-01-2021 and GRTIN-IRG-16-2021) for support of crystallographic studies. The use of the NCS X-ray crystallographic Service at the University of Southampton, UK, for collecting the intensity data and the valuable assistance of the staff there is gratefully acknowledged.

References

1 S. Burley and G. Petsko, *Science*, 1985, **229**, 23–28.

2 K. Müller-Dethlefs and P. Hobza, *Chem. Rev*., 2000, **100**, 143–167.

3 E. A. Meyer, R. K. Castellano and F. Diederich, *Angew. Chem. Int. Ed*., 2003, **42**, 1210–1250.

4 H.-J. Schneider, *Angew. Chem. Int. Ed*., 2009, **48**, 3924–3977.

5 R. W. Newberry and R. T. Raines, *ACS Chem. Biol*., 2019, **14**, 1677–1686.

6 C. A. Hunter and J. K. M. Sanders, *J. Am. Chem. Soc*., 1990, **112**, 5525–5534.

7 F. Cozzi, M. Cinquini, R. Annunziata, T. Dwyer and J. S. Siegel. *J. Am. Chem. Soc*., 1992, **114**, 5729–5733.

8 E. R .T. Tiekink and J. Zukerman-Schpector, *The importance pi-interactions in crystal engineering: Frontiers in Crystal Engineering*, John Wiley & Sons, Ltd, 2012.

9 J. K. Klosterman, Y. Yamauchi and M. Fujita, *Chem. Soc. Rev*., 2009, **38**, 1714–1725.

10 M. Nishio, *CrystEngComm*, 2004, **6**, 130–156.

11 E. C. Lee, D. Kim, P. Jurecka, P. Tarakeshwar, P. Hobza and K. S. Kim, *J. Phys. Chem. A*, 2007, **111**, 3446–3457.

12 D. B. Ninković, G. V. Janjić, D. Ž. Veljković, D. N. Sredojević, S. D. Zarić, *ChemPhysChem*, 2011, **12**, 3511–3514.

13 S. E. Wheeler, *Acc. Chem. Res.*, 2013, **46**, 1029–1038.

14 L.-J. Riwar, N. Trapp, B. Kuhn and F. Diederich, *Angew. Chem., Int. Ed.*, 2017, **56**, 11252–11257.

15 J. M. Živković, I. M. Stanković, D. B. Ninković and S. D. Zarić, *Cryst. Gowth Des*. 2020, 20, 1025–1034.

16 J. M. Živković, I. M. Stanković, D. B. Ninković and S. D. Zarić, *Cryst. Growth Des*., 2021, **21**, 1898–1904.

17 K. S. Kim, S. Karthikeyan and N. J. Singh, *J. Chem. Theory Comput*., 2011, **7**, 3471–3477.

18 D. B. Ninković, D. Z. Vojislavljević-Vasilev, V. B. Medaković, M. B. Hall, E. N. Brothers and S. D. Zarić, *Phys. Chem. Chem. Phys*., 2016, **18**, 25791–25795.

19 D. B. Ninković, J. P. Blagojević Filipović, M. B. Hall, E. N. Brothers, S. D. Zarić, *ACS Cent. Sci*. 2020, **6**, 420–425.

20 S. V. Baykov, A. S. Mikherdov, A. S. Novikov, K. K. Geyl, M. V. Tarasenko, M. A. Gureev and V. P. Boyarskiy, *Molecules*, 2021, **26**, 5672.

21 L. M. Salonen, M. Ellermann and F. Diederich, *Angew. Chem. Int. Ed*., 2011, **50**, 4808–4842.

22 M. Juhás and J. Zitko, *J. Med. Chem*., 2020, **63**, 8901–8916.

23 M. M. Herav and V. Zadsirjan, *RSC Adv*., 2020, **10**, 44247–44311.

24 E. G. Hohenstein and C. D. Sherrill, *J. Phys. Chem. A*, 2009, **113**, 878–886.

25 D. B. Ninković, G. V. Janjić and S. D. Zarić, *Cryst. Growth Des*., 2012, **12**, 1060–1063.

26 I. Geronimo, E. C. Lee, N. J. Singh and K. S. Kim, *J. Chem. Theory Comput*., 2010, **6**, 1931–1934.

27 D. B. Ninković, J. M. Andrić and S. D. Zarić, *ChemPhysChem*, 2013, **14**, 237–243.

28 I. F. Perepichka and D. F. Perepichka, *Handbook of thiophene-based materials: Applications in organic electronics and photonics*, John Wiley & Sons, 2009.

29 S. Pathania, R. K. Narang, and R. K. Rawal, *Eur. J. Med. Chem*., 2019, **180**, 486–508.

30 R. Mishra, N. Sachan, N. Kumar, I. Mishra and P. Chand, *J. Heterocycl. Chem*., 2018, **55**, 2019–2034.

31 M. Krátký and J. Vinsova, Curr. *Top. Med. Chem*., 2016, **16**, 2921–2952.

32 R. M. D. da Cruz, F. J. B. Mendonça-Junior, N. B. de Meló, L. R. S. A. de Araújo, R. N. de Almeida and R. O. de Moura, *Pharmaceuticals*, 2021, **14**, 692.

33 N. V. Bhilare, P. B. Auti, V. S. Marulkar and V. J. Pise, *Mini Revs. Med. Chem*., 2021, **21**, 217–232.

34 C. Capelini, K. R. de Souza, J. M. C. Barbosa, K. Salomão, P. A. Sales Junior, S. M. F. Murta, S. M. S. V. Wardell, J. L. Wardell, E. F. da Silva and S. A. Carvalho, *Med. Chem. Res*., 2021, **30**, 1703–1712.

35 S. K. Seth, V. S. Lee, J. Yana, S. M. Zain, A. C. Cunha, V. F. Ferreira, A. K. Jordão, M. C. B. V. de Souza, S. M. S. V. Wardell, J. L. Wardell and E. R. T. Tiekink, *CrystEngComm*, 2015, **17**, 2255–2266.

36 A. C. Pinheiro, T. C. M. Nogueira, C. França da Costa, C. Lourenço, J. N. Low, J. L. Wardell, S. M. S. V. Wardell and M. V. N. de Souza, *Z. Naturforsch. B*, 2020, **75**, 1011–1028.

37 L. N. F. Cardoso, M. L. F. Bispo, C. R. Kaiser, J. L Wardell, S. M. S. V. Wardell, M. C. S. Lourenço, F. A. F. M. Bezerra, R. P. P. Soares, M. N. Rocha, M. V. N. de Souza, *Arch. Pharm*., 2014, **347**, 432–448.

38 L. N. F. Cardoso, T. C. M. Nogueira, C. R. Kaiser, J. L. Wardell, S. M. S. V. Wardell and M. V. N. de Souza, *Mediterr. J. Chem*., 2016, **5**, 356–366.

39 L. N. F. Cardoso, T. C. M. Nogueira, F. A. R. Rodrigues, A. C. A. Oliveira, M. C. S. Luciano, C. Pessoa and M. V. N. de Souza, , *Med. Chem. Res*., 2017, **26**, 1605–1608.

40 L. N. F. Cardoso, T. C. M. Noguiera, C. R. Kaiser, J. L. Wardell, S. M. S. V. Wardell and M. V. N. de Souza, *Z. Kristallogr. Cryst. Mater*., 2016, **231**, 167–178.

41 R. W. W. Hooft, COLLECT. Nonius BV, Delft, The Netherlands, 1998.

42 Z. Otwinowski, W. Minor, Methods in Enzymology, in: C.W. Carter Jr, R.M. Sweet (Eds.), Macromolecular Crystallography, Part A, vol. 276, Academic Press, New York, 1997, pp. 307–326.

43 G. M. Sheldrick, SADABS. Bruker AXS Inc., Madison, Wisconsin, USA, 2007.

44 G. M. Sheldrick, *Acta Crystallogr., Sect. A: Found. Crystallogr*., 2008, **64**, 112–122.

45 G. M. Sheldrick, *Acta Crystallogr., Sect. B: Struct. Sci., Cryst. Eng. Mater*., 2015, **71**, 3–8.

46 L. J. Farrugia, *J. Appl. Crystallogr*., 2012, **45**, 849–854.

47 A. L. Spek, *Acta Crystallogr., Sect. E: Crystallogr. Commun*., 2020, **76**, 1–11.

48 K. Brandenburg, DIAMOND, Crystal Impact GbR, Bonn, Germany, 2006.

49 A. D. Becke, *J. Chem. Phys.*, 1993, **98**, 5648–5652.

50 F. Weigend and R. Ahlrichs, *Phys. Chem. Chem. Phys*., 2005, **7**, 3297–3305.

51 F. Weigend, *Phys. Chem. Chem. Phys*., 2006, **8**, 1057–1065.

52 M. J. Frisch, G. W. Trucks, H. B. Schlegel, G. E. Scuseria, M. A. Robb, J. R. Cheeseman, G. Scalmani, V. Barone, G. A. Petersson, H. Nakatsuji, X. Li, M. Caricato, A. V. Marenich, J. Bloino, B. G. Janesko, R. Gomperts, B. Mennucci, H. P. Hratchian, J. V. Ortiz, A. F. Izmaylov, J. L. Sonnenberg, D. Williams-Young, F. Ding, F. Lipparini, F. Egidi, J. Goings, B. Peng, A. Petrone, T. Henderson, D. Ranasinghe, V. G. Zakrzewski, J. Gao, N. Rega, G. Zheng, W. Liang, M. Hada, M. Ehara, K. Toyota, R. Fukuda, J. Hasegawa, M. Ishida, T. Nakajima, Y. Honda, O. Kitao, H. Nakai, T. Vreven, K. Throssell, J. A. Montgomery, Jr., J. E. Peralta, F.

Ogliaro, M. J. Bearpark, J. J. Heyd, E. N. Brothers, K. N. Kudin, V. N. Staroverov, T. A. Keith, R. Kobayashi, J. Normand, K. Raghavachari, A. P. Rendell, J. C. Burant, S. S. Iyengar, J. Tomasi, M. Cossi, J. M. Millam, M. Klene, C. Adamo, R. Cammi, J. W. Ochterski, R. L. Martin, K. Morokuma, O. Farkas, J. B. Foresman and D. J. Fox, Gaussian 16, Gaussian Inc., Wallingford CT, 2016.

53 M. J. Turner, J. J. McKinnon, S. K. Wolff, D. J. Grimwood, P. R. Spackman, D. Jayatilaka and M. A. Spackman, CrystalExplorer17, University of Western Australia, Crawley WA, 2017.

54 S. L. Tan, M. M. Jotani and E. R. T. Tiekink, *Acta Crystallogr. Sect. E: Crystallogr. Commun.*, 2019, **75**, 308–318.

55 M. A. Spackman and D. Jayatilaka, *CrystEngComm*, 2009, **11**, 19–32.

56 R. Ditchfield, W. J. Hehre and J. A. Pople, *J. Chem. Phys.*, 1971, **54**, 724–728.

57 W. J. Hehre, R. Ditchfield and J. A. Pople, *J. Chem. Phys.*, 1972, **56**, 2257–2261.

58 D. Jayatilaka and D. J. Grimwood, *Comput. Sci. – ICCS*, 2003, **4**, 142–151.

59 C. F. Mackenzie, P. R. Spackman, D. Jayatilaka and M. A. Spackman, *IUCrJ*, 2017, **4**, 575–587.

60 E. D. Glendening, A. E. Reed, J. E. Carpenter and F. Weinhold, NBO Version 3.1, University of Wisconsin, Madison, 1998.

61 A. E. Reed, L. A. Curtiss and F. Weinhold, *Chem. Rev.*, 1988, **88**, 899–926.

62 T. Lu and F. Chen, *J. Comput. Chem.*, 2012, **33**, 580–592.

63 R. F. W. Bader, *Atoms in Molecules: A Quantum Theory*, Oxford University Press, Oxford, 1990.

64 R. F. W. Bader, *Chem. Rev.*, 1991, **91**, 893–928.

65 R. F. W. Bader, *J. Phys. Chem. A*, 1998, **102**, 7314–7323.

66 E. R. Johnson, S. Keinan, P. Mori-Sánchez, J. Contreras-García, A. J. Cohen and W. Yang, *J. Am. Chem. Soc.*, 2010, **132**, 6498–6506.

67 J. Contreras-García, E. R. Johnson, S. Keinan, R. Chaudret, J.-P. Piquemal, D. N. Beratan and W. Yang, *J. Chem. Theory Comput.*, 2011, **7**, 625–632.

68 W. Humphrey, A. Dalke and K. Schulten, *J. Mol. Graph*., 1996, **14**, 33–38.

69 G. Palla, G. Predieri, P. Domiano, C. Vignali and W. Turner, *Tetrahedron*, 1986, **42**, 3649–3654.

70 V. V. Syakaev, S. N. Podyachev, B. I. Buzykin, S. K. Latypov, W. D. Habicher and A. I. Konovalov, *J. Mol. Struct*., 2006, **788**, 55–62.

71 O. Ünsal-Tan, K. Özden, A. Rauk and A. Balkan, *Eur. J. Med. Chem*., 2010, **45**, 2345–2352.

72 M. Nakka, M. S. Begum, B. F. M. Varaprasad, L. V. Reddy, A. Bhattacharya, M. Helliwell, A. K. Mukherjee, S. S. Beevi, L. N. Mangamoori, K. Mukkanti and S. Pal, *J. Chem. Pharm. Res.*, 2010, **2**, 393–409.

73 L. Mazur, K. N. Jarzembska, R. Kamiński, K. Woźniak, E. Pindelska and M. Zielińska-Pisklak, *Cryst. Growth Des.*, 2014, **14**, 2262–2281.

74 A. Bondi, *J. Phys. Chem*., 1964, **68**, 441–451.

75 C. Janiak, *J. Chem. Soc., Dalton Trans*., 2000, 3885–3896.

76 J. S. Murray, P. Lane, T. Clark, K. E. Riley and P. Politzer, *J. Mol. Model*. 2012, **18**, 541−548.

77 H. Wang, C. Li, W. Wang and W. J. Jin, *Phys. Chem. Chem. Phys*., 2015, **17**, 20636−20646.

78 P. Politzer, J. S. Murray, and T. Clark, *Phys. Chem. Chem. Phys*., 2021, **23**, 16458−16468.

79 S. Scheiner, *J. Phys. Chem. A*, 2021, **125**, 6514−6528.

80 C. R. Groom, I. J. Bruno, M. P. Lightfoot and S. C. Ward, *Acta Crystallogr., Sect. B: Struct. Sci., Cryst. Eng. Mater*., 2016, **72**, 171–179.

81 I. J. Bruno, J. C. Cole, P. R. Edgington, M. Kessler, C. F. Macrae, P. McCabe, J. Pearson and R. Taylor, *Acta Crystallogr., Sect. B: Struct. Sci., Cryst. Eng. Mater*., 2002, **58**, 389–397.

82 H. S. Yathirajan, B. Narayana, M. T. Swamy, B. K. Sarojini and M. Bolte, *Acta Crystallogr., Sect. E: Cryst. Commun.*, 2008, **64**, o119.

83 M. M. Naseer, M. Hussain, A. Bauzá, K. M. Lo and A. Frontera, *ChemPlusChem*, 2018, **83**, 881–885.

84 D. Sadhukhan, M. Maiti, G. Pilet, A. Bauzá, A. Frontera and S. Mitra, *Eur. J. Inorg. Chem.*, 2015, 1958–1972.

85 R. A. Howie, M. V. N. de Souza, A. Pinheiro, C. R. Kaiser, J. L. Wardell and S. M. S. V. Wardell, *Z. Kristallogr. Cryst. Mater*., 2011, **226**, 483–491.

86 T. Vu Quoc, L. Nguyen Ngoc, D. Tran Thi Thuy, M. Vu Quoc, T. Vuong Nguyen, Y. Oanh Doan Thi and L. Van Meervelt, *Acta Crystallogr., Sect. E: Cryst. Commun.*, 2019, **75**, 1090–1095.

87 A. S. Praveen, J. P. Jasinski, A. C. Keeley, H. S. Yathirajan and B. Narayana, *Acta Crystallogr., Sect. E: Cryst. Commun.*, 2012, **68**, o3435.

88 R. Kant, V. K. Gupta, K. Kapoor, S. Samshuddin, B. Narayana and B. K. Sarojini, *Acta Crystallogr., Sect. E: Cryst. Commun.*, 2012, **68**, o2923–o2924.

89 J. S. Foster, J. M. Żurek, N. M. S. Almeida, W. E. Hendriksen, V. A. A. le Sage, V. Lakshminarayanan, A. L. Thompson, R. Banerjee, R. Eelkema, H. Mulvana, M. J. Paterson, J. H. van Esch and G. O. Lloyd, *J. Am. Chem. Soc*., 2015, **137**, 14236–14239.

90 J. Xu, Y.-Q. Shu and P. Hu, *Z. Kristallogr. - New Cryst. Struct*., 2011, **226**, 63–64.

91 X.-F. Meng, W.-N. Li and J.-J. Ma, *J. Chil. Chem. Soc.*, 2014, **59**, 2647–2651.

92 Q.-L. Deng, M. Yu, X. Chen, C.-H. Diao, Z.-L. Jing and Z. Fan, *Acta Crystallogr., Sect. E: Cryst. Commun.*, 2005, **61**, o2545–o2546.

93 H. S. Naveenkumar, A. Sadikun, P. Ibrahim, J. H. Goh and H.-K. Fun, *Acta Crystallogr., Sect. E: Cryst. Commun.*, 2010, **66**, o3017–o3018.

94 S. Jiajaroen, K. Chainok and F. Kielar, *Acta Crystallogr., Sect. E: Cryst. Commun.*, 2017, **73**, 1151–1153.

95 S. Goswami, A. K. Das, K. Aich, A. Manna, H.-K. Fun and C. K. Quah, *Supramol. Chem.*, 2014, **26**, 94–104.

96 S. Ta, M. Ghosh, N. Salam, J. Das, M. Islam, P. Brandão, V. Félix, J. Sanmartin and D. Das, *Appl. Organomet. Chem.*, 2020, **24**, e5823.

97 N. Wang, J.-P. Li and Y.-L. Pu, *Chin. J. Struct. Chem.*, 2007, **26**, 547–550.

98 Y. Nie, *Acta Crystallogr., Sect. E: Struct. Cryst. Commun.*, 2008, **64**, o471.

99 X. Yu, Y.-F. Zhao, Y. Qin, J. Yan and Y.-F. Chen, *Z. Kristallogr.-New Cryst. Struct.*, 2019, **234**, 1039–1041.

100 G.-B. Cao, *Acta Crystallogr., Sect. E: Cryst. Commun.*, 2009, **65**, o2086.

101 T.-Y. Li and B.-B. Li, *Acta Crystallogr., Sect. E: Cryst. Commun.*, 2011, **67**, o383.

102 S. Sharma, M. S. Hundal, A. Walia, V. Vanita and G. Hundal, *Org. Biomol. Chem.*, 2014, **12**, 4445–4453.

103 D. R. Richardson and P. V. Bernhardt, *J. Biol. Inorg. Chem.*, 1999, **4**, 266–273.

104 L. M. F. Gomes, R. P. Vieira, M. R. Jones, M. C. P. Wang, C. Dyrager, E. M. Souza-Fagundes, J. G. Da Silva, T. Storr and H. Beraldo, *J. Inorg. Biochem.*, 2014, **139**, 106–116.

105 B. Joseph, N. R. Sajitha, M. Sithambaresan, E. B. Seena and M. R. P. Kurup, *Acta Crystallogr., Sect. E: Cryst. Commun.*, 2015, **71**, o826–o827.

106 J.-T. Lei, Y.-X. Jiang, L.-Y. Tao, S.-S. Huang and H.-L. Zhang, *Acta Crystallogr., Sect. E: Cryst. Commun.*, 2008 **64**, o909.

107 W. A. Yehye, A. Ariffin and S. W. Ng, *Acta Crystallogr., Sect. E: Cryst. Commun.*, 2008 **64**, o1452.

108 N. Md. Lair, H. Md. Ali and S. W. Ng, *Acta Crystallogr., Sect. E: Cryst. Commun.*, 2009 **65**, o189.

109 S. M. S. V. Wardell, J. L. Wardell, J. N. Low, C. Glidewell and M. V. N.de Souza, *Acta Crystallogr., Sect. C: Cryst. Struct. Chem.*, 2007, **63**, o42–o44.

110 P. Yang, H. Chen, Z.-Z. Wang, L.-L. Zhang, D.-D. Zhang, Q.-S. Shi and X.-B. Xie, *J. Inorg. Biochem*., 2020, **213**, 111248.

111 S. Mittapalli, D. S. Perumalla, J. B. Nanubolu and A. Nangia, *IUCrJ*, 2017, **4**, 812–823.

112 D.-X. Wu, J. Sun and M.-Z. Huang, *Z. Kristallogr. - New Cryst. Struct.*, 2009, **224**, 227–228.

113 H.-B. Ma, S.-S. Huang and Y.-P. Diao, *Acta Crystallogr., Sect. E: Cryst. Commun.*, 2008, **64**, o210.

114 L.-W. Xue, Y.-J. Han, C.-J. Hao, G.-Q. Zhao and Q.-R. Liu, *Acta Crystallogr., Sect. E: Cryst. Commun.*, 2008, **64**, o1938.

115 S. M. S. V. Wardell, M. V. N. de Souza, J. L. Wardell, J. N. Low and C. Glidewell, *Acta Crystallogr., Sect. C: Struct. Chem.*, 2005, **61**, o683–o689.

116 E. Tecer, N. Dege, A. Zülfikaroglu, N. Senyüz and H. Batil, *Acta Crystallogr., Sect. E: Cryst. Commun.*, 2010, **66**, o3369–o3370.

117 L. Wang, *Z. Kristallogr. - New Cryst. Struct.*, 2019, **234**, 1249-1250.

118 H.-K. Fun, C. K. Quah, P. C. Shyma, B. Kalluraya and J. H. S. Vidyashree, *Acta Crystallogr., Sect. E: Cryst. Commun.*, 2012, **68**, o2122.

119 J. Horkaew, S. Chantrapromma and H.-K. Fun, *Acta Crystallogr., Sect. E: Cryst. Commun.*, 2011, **67**, o2985.

120 Y.-Z. Wang, M.-D. Wang, Y.-P. Diao and Q. Cai, *Acta Crystallogr., Sect. E: Cryst. Commun.*, 2008, **64**, o668.

121 T. Kundu, J. Wang, Y. Cheng, Y. Du, Y. Qian, G. Liu and D. Zhao, *Dalton Trans.*, 2018, **47**, 13824–13829.

122 W.-M. Zhang, G.-H. Sheng and Z. You, *Asian J. Chem*., 2014, **26**, 8118–8122.

123 M. Wu, D. Wang, J.-Q. Zheng, D.-C. Fang, L.-P. Jin and X.-J. Zheng, *Chem. Sel*., 2018, **3**, 2174–2180.

124 Y.-P. Diao, S.-S. Huang, J.-K. Zhang and T.-G. Kang, *Acta Crystallogr., Sect. E: Cryst. Commun.*, 2008, **64**, o470.

125 P. V. Bernhardt, P. Chin, P. C. Sharpe and D. R. Richardson, *Dalton Trans.*, 2007, 3232–3244.

126 H. H. Monfared, R. Bikas and P. Mayer, *Acta Crystallogr., Sect. E: Cryst. Commun*., 2010, **66**, o236–o237.

127 Y.-X. Zhang, *Acta Crystallogr., Sect. E: Cryst. Commun.*, 2008, **64**, o2208.

128 M. C. Vineetha, M. Sithambaresan, Y. S. Nair, M. R. Prathapachandra Kurup, *Inorg. Chim. Acta*, 2019, **419**, 93–104.

129 P. Muthukumar, M. Surya, M. Pannipara, A. G. Al-Sehemi, D. Moon and S. P. Anthony, *Chem. Sel.*, 2020, **5**, 3295–3302.

130 Y.-F. Sun, Z.-Y. Chen, Y.-L. Liu, N. Li, J.-K. Li and H.-C. Song, *Dyes Pigm.*, 2012, **95**, 512–522.

131 H. Kargar, R. Kia and M. N. Tahir, *Acta Crystallogr., Sect. E: Cryst. Commun.*, 2012, **68**, o2321–o2322.

132 Y. Zhang, S.-P. Zhang, Y.-Y. Wu and S.-C. Shao, *Acta Crystallogr., Sect. E: Cryst. Commun.*, 2006, **62**, o119–o120.

133 E. Wyrzykiewicz, A. Błaszczyk and I. Turowska-Tyrk, *Bull. Pol. Acad. Sci., Chem.*, 2000, **48**, 212-229.

134 J. N. Low and J. L. Wardell, Private Communication to the Cambridge Structural Database, Refcode ROGFEZ01, 2018.

135 D. T. G. Gonzaga, F. C. da Silva, V. F. Ferreira, J. L. Wardell and S. M. S. V. Wardell, *J. Braz. Chem. Soc.*, 2016, **27**, 2322–2333.

136 N. Dege, N. Şenyüz, H. Bati, N. Günay, D. Avcı, Ö. Tamer and Y. Atalay, *Spectrochim. Acta Part A Mol. Biomol*, 2014, **120**, 323–331.

137 U. Saha, B. Das, M. Dolai, R. J. Butcher and G. S. Kumar, *ACS Omega*, 2020, **5**, 18411–18423.

138 M. W., D.-D. Yang, H.-W. Zheng, Q.-F. Liang, J.-B. Li, Y. Kang, S. Li, C. Jiao, X.-J. Zheng and L.-P. Jin, *Dalton Trans*, 2021, **50**, 1507–1513.

139 V. Felix, Private Communication to the Cambridge Structural Database, Refcode ZOJSAV, 2019.

140 L.-N. Zhu, C.-Q. Li, X.-Z. Li and R. Li, *Acta Crystallogr., Sect. E: Cryst. Commun.*, 2006, **62**, o4603–o4605.

141 X. Li, J. Qiao, S. W. Chee, H.-S. Xu, X. Zhao, H. S. Choi, W. Yu, S. Y. Quek, U. Mirsaidov and K. P. Loh, *J. Am. Chem. Soc.*, 2020, **142**, 4932–4943.

142 V. Arumugam, C. Shalini, N. Dharmaraj, W. Kaminsky and R. Karvembu, *Eur. J. Inorg. Chem.*, 2019, 3869–3882.

143 Y.-P. Diao, J.-K. Zhang, S.-Q. Xie and T.-G. Kang, *Acta Crystallogr., Sect. E: Cryst. Commun.*, 2007, **63**, o4908.

144 J. T. Mague, S. K. Mohamed, M. Akkurt, H. Potgieter and M. R. Albayati, *Acta Crystallogr., Sect. E: Cryst. Commun.*, 2014, **70**, o612.

145 C.-L. Du, *Acta Crystallogr., Sect. E: Cryst. Commun.*, 2009 **65**, o29.

146 Y. Lei, T.-Z. Li, C. Fu, X.-L. Guan and Y. Tan, *J. Chem. Crystallogr.*, 2011, **41**, 1707.

147 H.-Y. Zhu, *Asian J. Chem.*, 2012, **24**, 558–560.

148 O. Pouralimardan, A.-C. Chamayou, C. Janiak and H. Hosseini-Monfared, *Inorg. Chim. Acta*, 2007, **360**, 1599–1608.

149 S. Zhao, L. Li, X. Liu, W. Feng and X. Lu, *Acta Crystallogr., Sect. E: Cryst. Commun.*, 2012, **68**, o2040.

150 H. A. Arjun, G. N. Anil Kumar, R. Elancheran and S. Kabilan, *Acta Crystallogr., Sect. E: Cryst. Commun.*, 2020, **76**, 132–136.

151 A. S. Mahadevi and G. N. Sastry, *Chem. Rev.*, 2016, **116**, 2775–2825.

152 Y.-J. Wei and E.-W. Wang, *J. Struct. Chem.*, 2011, **52**, 775.

153 L. Tom, V. A. Smolenski, J. P. Jasinski and M. R. Prathapachandra Kurup, ChemRxiv, 2018, https://doi.org/10.26434/chemrxiv.6489425.